JOURNAL OF MATERIALS SCIENCE 7 (1972) 1161–1167

Creep of germanium

G. CHAUDHRI, P. FELTHAM
Brunel University, Uxbridge, London, England

Isothermal creep, as well as the response to incremental stress and temperature changes, were studied in germanium single crystals oriented for double slip, in the range 470 to 700°C. The stress-sensitivity of the compressive creep rate $\partial \ln \dot{\epsilon} / \partial \ln \sigma$ is numerically close to 3 at low strains, but increases appreciably with deformation. This effect, and a similar strain dependence of the activation energy as determined by thermal cycling, are explained in terms of the curvature of the creep curves on the basis of Boltzmann's superposition principle. The Peierls barrier seems to be an important obstacle to dislocation movement at relatively low temperatures, when S-shaped creep curves are observed. Other barriers, with greater heights, seem to become increasingly effective above about 550°C. Although dislocation loops, and the formation and break-up of dipoles were observed by TEM, recovery mechanisms involving self-diffusion did not appear to make a substantial contribution to the creep within the range of temperatures used.

1. Introduction

The interest in semiconductor materials, following the discovery of the transistor in 1948, and the ensuing availability of germanium and silicon crystals of high purity and crystallographic perfection, stimulated researches on their mechanical properties in the last two decades. An extensive review of the work on the plasticity and the creep of crystals having the diamond lattice was published in 1968 by Alexander and Haasen [1]. Further work on the creep of germanium crystals by Berner and Alexander [2] appeared at about the same time, and was followed by a spectrum of work on the mechanical response of crystals with the diamond structure. This included measurements of the velocity of dislocations [3-5], work on the character of the energy barrier to their motion and on the stress dependence of their velocity [6], as well as observations of dislocation sources activated at high temperatures [7].

Several investigations of dislocation structures developing in the course of creep [8-11] and deformation [12] have been made by transmission electron microscopy (TEM) in recent years, complementing earlier work [13, 14]. Except in relation to the new interpretation of the mechanism by which dislocations in the diamond lattice overcome the Peierls barrier [6] no new basic modifications have however been proposed to the semi-empirical model of the creep process outlined by Alexander and Haasen [1]. The TEM observations have confirmed the frequent occurrence of dipoles in crept crystals; their function in the creep process has not however been fully established.

The characteristic S-shaped curves obtained with such crystals are described by Alexander and Haasen [1] by a semi-empirical expression; in its derivation they took into account the observations that early in the creep the crystal "fills up" with dislocations, and that the concommitant work-hardening results in a "negative feedback", reducing the rate of generation and the mean velocity of dislocations as the deformation proceeds.

The assumption of a linear stress dependence of the dislocation velocity, and the use of an activation energy equal to that governing the "lattice friction" associated with the Peierls potential, i.e. 1.6 eV in the case of germanium, are consistent with the prevailing view that this lattice friction is rate controlling in creep. An energy barrier would however be expected to become "transparent" in creep when the temperature exceeds about $u_0/25k$ which, for $u_0 = 1.6$ eV, is about 500°C. There are in fact some indications [15] that higher barriers do occur. Also, some empirical assumptions involved in the derivation, e.g. the use of an "effective

stress" which is uniform throughout the crystal, and additive, i.e. equal to the difference between the applied stress and an internal "back stress" proportional to the square root of the dislocation density, is unrealistic [16], as is clear also from an inspection of the heterogeneous dislocation structure in micrographs obtained by TEM. The difficulty is not removed on using a periodic rather than a constant "back stress" [17].

If the structural heterogeneity is taken into account statistically then, as shown in a more recent treatment of creep [18], the main features of the process can be described, and the S-shape of the curves can be explained, without recourse to a constant or periodic "back stress". In view of the "slow" movement of dislocations in the creep of crystals having the diamond lattice, compared with materials with a relatively low Peierls potential, creep in germanium seemed particularly suitable for re-examination in the light of this "diffusional" stochastic model [18]; to carry out such a study was in fact the main object of the present work. More specifically, it was intended, firstly, to examine the isothermal creep of germanium crystals, including the stress sensitivity of the strain-rate as determined by incremental loading, the activation energy as determined by thermal cycling and, secondly, to investigate the structure of crept crystals by TEM, and to discuss the theoretical significance of the experimental results.

The "incremental" methods referred to are difficult to use with small crystals of low thermal conductivity, as there are numerous sources of error and, except in [15], they do not seem to have been used with semiconductors. It was therefore essential to pay special attention to the problem of the sensitivity of measurement and to the elimination of errors arising, for example, in the course of thermal-cycling runs from thermal expansion in the equipment.

2. Experimental

The germanium crystals used were Sb-doped, with 7×10^{13} donors/cm^3, and an initial dislocation density of 3×10^3 cm^{-2}, measuring $0.4 \times 0.4 \times 1.0$ cm. They were oriented for double slip, with the long, "compression" axis along [1 1 0]; the rectangular faces were $(1\bar{1}1)$ and $(\bar{1}12)$. Initially the Schmid-factor for slip was 0.41.

Before being strained in compression, the crystals were polished mechanically and chemically, as recommended by Berner and Alexander [2]; the chemical polish served to remove the worked surface-layer to a depth of about 0.15 mm. Crystals had a mirror finish and, in general, emerged bright from the furnace after creep. Deformation in compression took place in a continuously evacuated chamber, the specimen being sandwiched between two ground zirconia rods. The diffusion pump was provided with a liquid-air trap, and a controlled leak of high-purity argon was used to dilute the residual air in the vacuum vessel; the vacuum, as measured by a Penning gauge, was 10^{-4} torr during runs. The end-faces of the crystals were lubricated with molybdenum sulphite to minimize barrelling; the latter effect was not however important, for compressive strains did not as a rule exceed about 4%. Strain was measured with an inductive transducer. Precautions taken to "eliminate" thermal expansion effects in strain measurements, and to assure accuracy of measurement and stability of temperature in thermal cycling experiments have been outlined before [19, 20]. Attainment of thermal equilibrium of the specimen following a rapid temperature change by 20°C, in the range of temperature used, was evaluated by two methods, assuming rather unfavourable conditions of heat transfer, i.e. by radiation only, and was found to take about 1½ min. Nevertheless, strain measurements made during the first 3 min after the change of the temperature within the furnace by 20°C were not used in calculations.

Crystals were allowed to cool in the furnace under load, and were then examined by optical and electron microscopy. Replicas and thin films were used; the films were made from slices cut parallel to active slip planes by a combination of mechanical polishing [21] and jet-machining [22].

3. Results and discussion

3.1. Isothermal creep curves

Creep curves obtained at a compressive stress $\sigma = 485$ kg/cm^2 at several temperatures, shown in Fig. 1, have the characteristic S-shape, except for that obtained at 580°C which, in common with the series obtained at 650°C at different stress levels (Fig. 2), is approximately logarithmic at first, and nearly linear later in the creep. The disappearance of the foot of the "S" indicates that the process of "fillling up" with dislocations is rather rapid, tending towards completion early in a run.

A solution for the creep rate, given by the

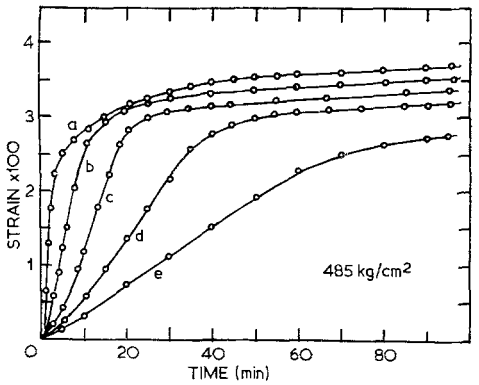

Figure 1 Creep isotherms at a compressive stress of 485 kg/cm². Temperatures corresponding to letters a, b, c, d, e were 580, 545, 520, 495 and 470°C respectively.

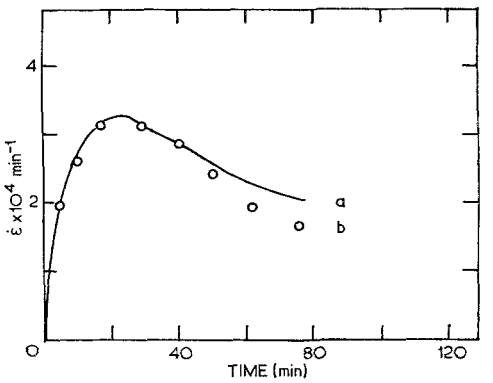

Figure 3 The strain-rate as a function of time as calculated from Equation 1 (curve a), and as obtained from curve "e" of Fig. 1 (curre b).

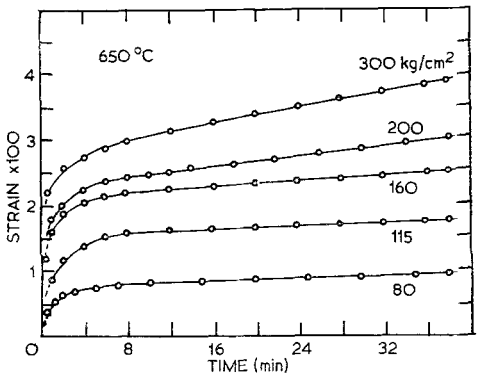

Figure 2 Creep isotherms at 650°C at various stresses, marked on the curves.

stochastic model of creep [18], which yields S-shaped creep cruves is

$$\epsilon = \epsilon_0[\mathrm{erf}(at^{-\frac{1}{2}}) - \mathrm{erf}(bt^{-\frac{1}{2}})], \qquad (1)$$

where $\dot{\epsilon}_0$, a and b are constant for a given isothermal creep test at constant stress. Their optimum values for the representation of an experimentally determined creep curve require some tedious calculation, and no attempt was made to determine the best fit in the evaluation of curve (a) in Fig. 3 from Equation 1; for the "rough" fit shown $\dot{\epsilon}_0 = 1.1 \times 10^{-3}$ min^{-1}, $a = 4.3$ min$^{\frac{1}{2}}$ and $b = 2.3$ min$^{\frac{1}{2}}$, The error, amounting to 15% at 75 min in relation to the points (b) obtained from curve "e" in Fig. 1, could probably be reduced with an optimized set of constants in Equation 1. The activation energy determined from the temperature dependence of the strain-rate at the inflexion points of the curves shown in Fig. 1 is 1.5 ± 0.1 eV, agreeing with the value of 1.65 eV obtained by Shea *et al.* [23] in the same manner under similar conditions. The curves do not however seem to converge at a common upper strain limit, which detracts rather from the reliability of this "slope" method in determining activation energies.

The parameters a and b in Equation 1 are proportional to $u_2 \exp(\frac{1}{2}u_2/kT)$ and $u_1 \exp(\frac{1}{2}u_1/kT)$ respectively [18], where u_2 and u_1 are the upper and lower limit of values of the activation energies which the energy-barrier distribution can comprise at any time during creep. The reason for the limitation of the spectrum to a band is apparent if one considers that "jumps" over barriers less than a certain height u_1 would have already become "exhausted" during the period required in loading the material to the level of the creep stress; similarly, jumps with retardation times significantly longer than the period over which appreciable creep takes place are assumed not to make a contribution to the strain-rate. Thus, apart from the mathematical convenience involved in practice, it is possible to truncate the physically possible range of u-values also at an upper limit u_2.

As a result of the temperature dependence of the parameters a and b, the initial, steep, part of the strain-rate curve (Fig. 3) approaches the ordinate as the creep temperature is increased. Eventually this part, and the foot in the strain-time curve corresponding to it, cease to be resolvable (Fig. 2). The initial part, as exemplified by the upper three curves in Fig. 1, are then nearly linear. An equation simpler than Equation 1 may then be used [18]. It is given by

$$\dot{\epsilon} = \nu\rho b^2 \exp(-u^*/kT) \,.\, [1 - (t/t_\infty)] \,, \qquad (2)$$

and is based on the assumption, somewhat idealized, that "filling-up" with dislocations is completed during the rapid, unresolvable, stage of deformation. The density ρ in Equation 2 is thus constant; it comprises all activatable dislocations or parts of dislocations which at the time of completion of loading are associated with barriers comprised within the range $\Delta u = u_2 - u_1$. The "characteristic" activation energy, equal to about 25 kT, is defined by $u^* = \frac{1}{2}(u_1 + u_2)$; the limiting retardation time, at which the strain-rate becomes equal to zero, and beyond which Equation 2 becomes inapplicable, is given by

$$t_\infty^{-1} = 2\alpha(kT/\Delta u) \sinh(\Delta u/kT) \,.\, \exp(-u^*/kT) \,, \qquad \ldots\ldots (3)$$

where α, like ν in Equation 2, are "atomic" frequencies.

On writing $\Delta u \propto \sigma - \sigma_y$, [18], and $\rho \propto (\sigma - \sigma_y)^2$, [24], one finds that for the near-linear part of the creep curves

$$\dot{\epsilon} \propto (\sigma - \sigma_y)^2 \exp(-u^*/kT) \,, \qquad (4)$$

but that the final strain, as attained at $t = t_\infty$, is much less dependent on either temperature or on "effective" stress $(\sigma - \sigma_y)$, as is readily seen from the relation

$$\epsilon(t_\infty) = \tfrac{1}{2}\dot{\epsilon}_0 \,.\, t_\infty \,, \qquad (5)$$

obtained from Equation 2, where $\dot{\epsilon}_0$ is the term outside the last bracket in Equation 2. Equation 2 also shows that it should be possible to obtain u^* from the temperature dependence of the slope of the "linear" parts of isobaric sets of creep curves, such as are shown in Fig. 1. The requirement $u^* \approx 25\,kT$ yields, for the mean temperature of 800 K, for the results in Fig. 1, $u^* = 1.65$ eV. Thus, although the same value appears to be associated with the activation energy controlling the dislocation velocity, the coincidence may be fortuitous in the sense that for the onset of significant dislocation movement the activation energy for migration would also have to satisfy a relation $u_m \approx 25\,kT$. At temperatures significantly above $u_m/25\,k$ barriers other than the lattice friction due to the Peierls field would however have to become effective, as the Peierls field would become "transparent". At such temperatures one should therefore expect $u^* > u_m$; this inference is in accord with observations by Bell and Bonfield [15].

The "high-temperature" creep curves, obtained at 650°C (Fig. 2) cannot be represented adequately by Equation 2. However, as before, a rather small stress-dependence of the creep is found. For strains in the sharply curved region extending to about 8 min, strains corresponding to a given time are found to be proportional to $(\sigma - 60)^{\frac{1}{2}}$, where the value $\sigma_y = 60$ kg/cm² is obtained graphically, by extrapolation of the σ/ϵ relation for fixed times. The "steady" creep rate, at times exceeding about 10 min, has a similar, weak, stress dependence.

3.2. Incremental methods

The activation energy as determined by temperature cycling was found to be 1.6 ± 0.1 eV in the steep, near-linear parts of the creep curves. In the upper, flat, parts higher values were obtained: 3.5 ± 0.3 eV. Fig. 4 shows such a section of a creep curve; the inset represents the region around the 3.5 eV point, enlarged ten times. The dotted lines, which are shown extrapolated, were used in determining the activation energy in this transition from 640 to 660°C.

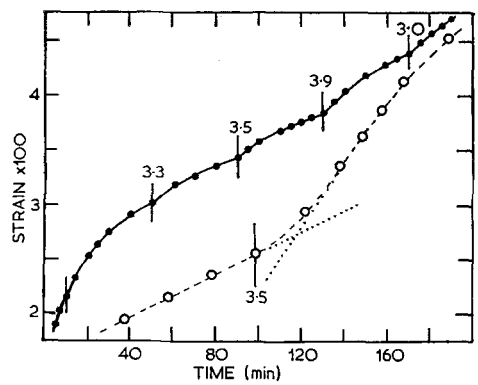

Figure 4 Determination of activation energies by thermal cycling in the upper part of a creep curve. Transitions were from 600 to 620, 620 to 640, 640 to 660, 660 to 680 and 680 to 700°C. The first reading, on the extreme left, was unreliable. Values in eV. The inset is enlarged × 10.

Values of the stress-sensitivity of the strain-rate, $\partial \ln \dot{\epsilon}/\partial \ln \sigma$, obtained with an incremental stress of ± 31 kg/cm² at a nominal stress of 436 kg/cm², at 500°C are shown in Fig. 5. The short lines at the points of transition indicate the sense in which the increment was made. The enlarged portion of the curve around the last "down cycling" point, magnified four times, shows the occurrence of an "incubation period". By contrast, due to loading on up-cycling transients were observed for a few seconds. These were ignored in the evaluation of the stress

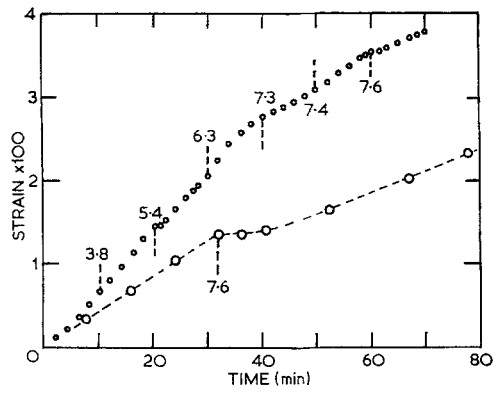

Figure 5 Determination of the stress-sensitivity of the compressive strain-rate $\partial \ln \dot{\epsilon}/\partial \ln \sigma$ by stress-cycling. The nominal stress was 436 kg/cm², the changes ± 31 kg/cm². $T = 500°C$. Inset magnification × 4.

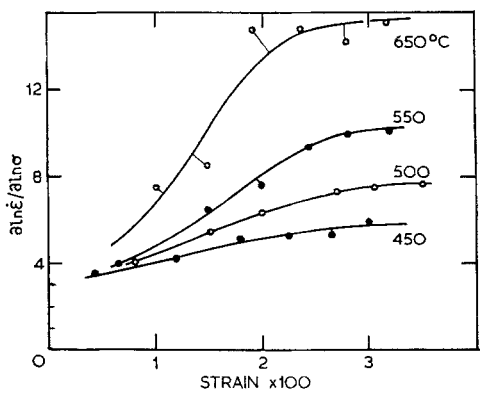

Figure 6 The stress-sensitivity of the strain-rate as determined by stress cycling, as function of strain and temperature.

sensitivity, which was evaluated from the nearly straight parts on both sides of the transition period, clearly visible, e.g. in the inset in Fig. 5. The dependence of the stress-sensitivity of the strain-rate on the compressive strain and on temperature is shown in Fig. 6.

We shall attempt to explain the significance of the results shown in Figs. 4 to 6 with the aid of Equation 2. Although it has been derived for specific boundary conditions, and is not therefore an equation of state, we shall nevertheless, at first, regard it as such for the present considerations. We shall also assume that $\Delta u/kT$ is sufficiently small to make t_∞, as given by Equation 3, effectively stress independent. The last bracket in Equation 2 is then dependent only on time and temperature.

In view of the linear relation between ϵ and ρ, the Boltzmann superposition principle may be used. Thus, if at a time $t = \theta$ the strain-rate is increased by $\Delta\dot{\epsilon}$ in an isothermal test, then

$$\Delta\dot{\epsilon} = \nu\Delta\rho \,.\, b^2 \exp(-u^*/kT)\left[1 - \frac{t-\theta}{t_\infty}\right]. \quad (6)$$

On dividing Equation 6 by Equation 2 ,using the relation $\rho \propto (\sigma - \sigma_y)^2$, and putting $t = \theta$, corresponding to the time at which the increment is made, one has, for positive stress increments, i.e. only for plastic strain,

$$\frac{\Delta \ln \dot{\epsilon}}{\Delta \ln \sigma} = \left[2\frac{\sigma}{\sigma - \sigma_y}\right] \cdot \frac{1}{1 - (\theta/t_\infty)}. \quad (7)$$

Now σ_y appropriate for the curve shown in Fig. 5 was not measured but, in view of its temperature dependence through an Arrhenius term $\exp(u^*/3\,kT)$, [1, 24] its value was determined to be 240 kg/cm², using $\sigma_y = 60$ kg/mc² at 650°C, obtained directly from the data in Fig. 2. Thus, referring to Fig. 5, where $\sigma = 436$ kg/cm², $\sigma/(\sigma - \sigma_y) = 2.2$, so that the magnitude of the bracketed term is 4.2 and, as $\theta \to t_\infty$ the stress-sensitivity would be expected to grow with time. This trend, as well as the numerical magnitude of the stress sensitivity are thus quite well accounted for even in terms of the rather simple model used. In the case of the uppermost curve in Fig. 6, $\sigma = 187$ kg/cm² and $\sigma_y = 60$ kg/cm²; the value of the bracketed term in Equation 7 is now close to 3.0, a plausible value in view of the trend of the curve at low strains.

Similarly, for a change in temperature

$$\Delta\dot{\epsilon} = \nu\rho b^2 \,.\, \Delta \exp(-u^*/kT) \,.\, \left[1 - \frac{t-\theta}{t'_\infty}\right] \quad (8)$$

where the "dash" on t'_∞ is to differentiate it from t_∞, the difference arising from the change in temperature. Again, as in the case of Equation 7, one finds for $t = \theta$,

$$-k\frac{\Delta \ln \dot{\epsilon}}{\Delta T^{-1}} = u^*\left[\frac{1}{1 - (\theta/t_\infty)}\right]. \quad (9)$$

The increase in the activation energy from about 1.6 eV early in the test, i.e. for $\theta/t_\infty \ll 1$, to over twice this value (Fig. 4), thus appears to have the same cause as the increase of the stress-sensitivity of the strain-rate (Figs. 5 and 6). In the latter figure the values are also seen to double approximately in the course of creep. The strain-dependence of both parameters does not therefore point to some fundamental change in the creep mechanism in the course of deformation; it appears to be largely a consequence of the

changing curvature of the creep curve. For a constant, time-independent creep-rate, the compilation of creep data by Balasubramanian and Li [25] shows that for germanium, silicon and indium antimonide the stress sensitivity of the creep rate is close to 3; this value is readily explained in terms of Equation 7.

3.3. Induction periods

The occurrence of transients and induction periods following small changes in parameters in incremental tests can be explained in terms of changes in the distribution of energy-barrier levels to dislocation movement [18]. We shall illustrate this with reference to transients.

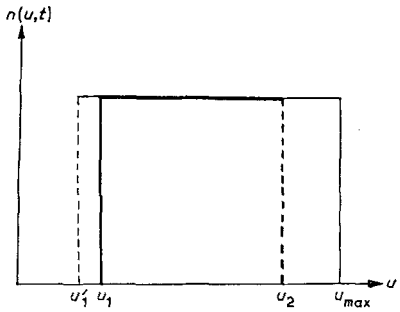

Figure 7 Displacement of the activation energy distribution $n(u, t)$ at a given time, due to the application of a stress increment to the crystal. The loss of "states" in the "low" energy strip $u_1' - u_1$ leads to transients. States to the right of u_2 are "frozen in".

In Fig. 7 we have represented the u-distribution at a given time by the "top hat" in which the region to the right of u_2 consists of inactive, "frozen-in" states, i.e. those unlikely to participate in creep during a run. A small increase in stress on the specimen will result in a more or less, bodily displacement of the "hat" to the left, e.g. by an amount $u_1 - u'_1$ indicated in the figure. States in the strip above the segment $u'_1 - u_1$ have rather low u-values, and will be used up rapidly, giving rise to the observed transients. Apart from any changes in the height or shape of the distribution, such as would have occurred during this period also in the absence of the incremental deformation, the *status-quo ante* is thus largely restored.

3.4. Microstructure

Characteristic features of the microstructure were, firstly, elongated dipoles, secondly, loops, which appear to have been formed through the

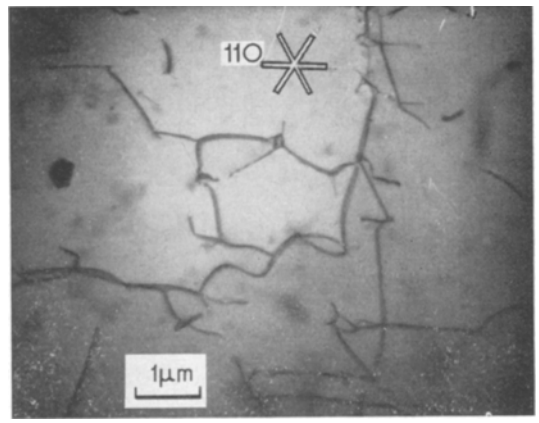

Figure 8 Loops, and bowing "S"-shaped dislocations indicative of the mode of formation of loops. Deformed 5% at 700°C; (111) plane.

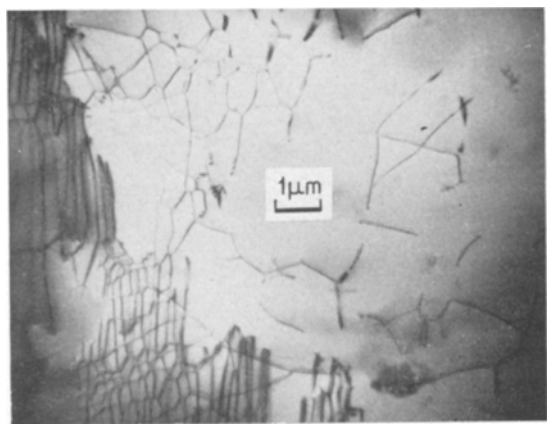

Figure 9 Networks in the (111) plane. Crystal deformed 5% at 720°C under a stress of 280 kg/cm². ⟨110⟩ approximately along the direction of the marker.

pinching-off of dipoles [26] and, finally, networks formed by dislocations belonging to the same glide plane (Figs. 8 and 9). Regular networks were not found below about 700°C; they appear to be a major source of strength when the Peierls field is no longer a dominant barrier to dislocation movement.

It appears likely that the shrinkage of dipole-generated loops contributes to recovery and, hence, may be responsible for the slow, steady, creep in evidence in Fig. 2 for example. Whether a diffusion controlled shrinkage occurred could not be established; an activation energy of about 3.1 eV would be expected to be rate controlling in such a process [19]. The movement of

dislocations into dipole configurations does however appear to be a mechanism which takes place, facilitating recovery through the reduction of internal stress fields.

4. Conclusions

The present results and considerations show that the principal features of the creep of germanium crystals can be interpreted satisfactorily in terms of the stochastic model proposed in [18]. The Peierls barrier seems an effective obstacle to dislocation movement at relatively low creep-temperatures; higher barriers seem to participate at high temperatures. This view finds some support in the literature [15]; the effectiveness of the dislocation network as a source of work-hardening in creep is also indicated by the relatively high stress levels at which the crystals oriented for double slip creep at a certain rate, compared with similar crystals oriented for single slip as used, for example, by Berner and Alexander [2]. The use of the Boltzmann superposition principle suggests that the high activation energies deduced by thermal cycling in the upper, plateau, stage of the creep curves may be an artefact, i.e. it does not, in all probability, correspond to recovery mechanisms other than those operative at lower strains.

That thermally activated shrinkage of dipoles may contribute to recovery cannot be excluded as a possibility, it was not however possible to establish the extent to which such a process contributed to the creep.

The parameter σ_y, appearing in Equation 4 for example, characterizes the width of the distribution of energy barriers to the movement of dislocations; it cannot be interpreted in terms of a "back stress" of fixed magnitude prevailing throughout the crystal.

References

1. H. ALEXANDER and P. HAASEN, *Solid State Physics* **22** (1968) 27.
2. K. BERNER and H. ALEXANDER, *Acta Metallurgica* **15** (1967) 933.
3. H. SCHAUMBURG, *Phys. Stat. Sol.* **40** (1970) K1.
4. V. I. NIKITENKO, M. M. MYSHLYAEV, and V. G. EREMENKO, "Dinamika Dislokatsii" (*Ak. Nauk. Ukr. SSR, Kharkov*, 1968) p. 84.
5. J. R. PATEL and P. E. FREELAND, *J. Appl. Phys.* **42** (1971) 3298.
6. P. FELTHAM, *Phys. Letts.* **33A** (1970) 239.
7. L. GERWARD, *Phys. Stat. Sol.* **2a** (1970) 797.
8. F. CALZECCHI, A. GARDINI, and P. GONDI, *Nuovo. Cim.* **50** (1967) 263.
9. V. F. MIUSKOV, "Dinamika Dislokatsii" (*Ak. Nauk. Ukr. SSR, Kharkov*, 1968) p. 204.
10. M. M. MYSHLYAEV, V. I. NIKITENKO, and V. I. NESTERENKO, *Phys. Stat. Sol.* **36** (1969) 89.
11. R. WAGATSUMA, K. SUMINO, W. UCHIDA, and S. YAMAMOTO, *J. Appl. Phys.* **42** (1970) 222.
12. K. KOJIMA and K. SUMINO, *Crystal Lattice Defects* **2** (1971) 147, 159.
13. D. B. HOLT and A. E. DANGOR, *Phil. Mag.* **8** (1963) 1921.
14. V. G. GOVORKOV, V. L. INDENBOM, V. S. PAPKOV, and V. R. REGAL, *Sov. Phys. Sol. State* **6** (1964) 802.
15. R. L. BELL and W. BONFIELD, *Phil. Mag.* **9** (1964) 9.
16. P. FELTHAM, *ibid* **21** (1970) 765.
17. R. LABUSCH, *Festkörperphysik* **8** (1968) 268.
18. P. FELTHAM, *Phys. Stat. Sol.* **30** (1968) 135.
19. D. BROWN, G. CHAUDHRI, and P. FELTHAM, *Phil. Mag.* **24** (1971) 213.
20. G. CHAUDHRI, Ph.D. Thesis (Brunel University, London 1971) p. 14.
21. B. A. IRVING, *Brit. J. Appl. Phys.* **12** (1961) 92.
22. G. R. BOOKER, and R. STICKLER, *ibid*, **13** (1962) 446.
23. M. M. SHEA, L. E. HENDRICKSON, and L. A. HELDT, *J. Appl. Phys.* **37**, (1966) 4572.
24. P. FELTHAM and G. CHAUDHRI, *Phys. Stat. Sol.* **7a** (1971) K59.
25. N. BALASUBRAMANIAN and J. C. M. LI, *J. Mater. Sci.* **5** (1970) 434.
26. P. HAASEN, *J. de Physique* **27** (1966) C3-31.

Received 19 January and accepted 27 March 1972.